A Study on the Modeling of Static Pressure Distribution of Wet Gas in Venturi

Peining Yu, Ying Xu, and Tao Zhang
School of Electrical and Automation Engineering, Tianjin University, Tianjin 300072, China

Zicheng Zhu
School of Mechanical and Aerospace Engineering, Nanyang Technological University, Singapore City 639798, Singapore

Xili Ba
PetroChina Planning and Engineering Institute, Beijing 100083, China

Jing Li
Natural Gas Dept., PetroChina Tarim Oilfield Company, Korla 841000, China

Zigeng Qin
Key Laboratory of Earth Exploration & Information Technology of Ministry of Education, Chengdu 610059, China

CCDE Geophysical Prospecting Company, Chengdu 610213, China

DOI 10.1002/aic.14657
Published online October 28, 2014 in Wiley Online Library (wileyonlinelibrary.com)

A model for gas–liquid annular and stratified flow through a standard Venturi meter is investigated, using the two-phase hydrokinetics theory. The one-dimensional momentum equation for gas has been solved in the axial direction of Venturi meters, taking into consideration the factors including the void fraction, the friction between the two phases and the entrainment in the gas core. The distribution of wet gas static pressure between the two pressure tapings of the Venturi meters has been modeled in the pressure range of 0.1–0.6 MPa. Compared with the experimental data, all the relative deviations of the predicted points by the model were within ±15%. As the model is less dependent on the specific empirical apparatus and data, it provides the basis for further establishing a flow measurement model of wet gas which will produce fewer biases in results when it is extrapolated. © 2014 American Institute of Chemical Engineers *AIChE J*, 61: 699–708, 2015

Keywords: wet gas flow, Venturi meter, pressure drop modeling

Introduction

As a specific subset of gas–liquid two-phase flow, wet gas widely exists in various manufacturing processes in industry. According to the definition of the technical report released by International Organization for Standards (ISO/TR11583),[1] wet gas refers to the two-phase flows of gas and liquid in which the flowing fluid mixture consists of gas in the region of more than 95% volume fraction. This definition is adopted in this study and all the experiment conditions were within this scope.

In 1797, the Italian physicist, Giouan Battista Venturi, described the relationship between the velocity and static pressure of the flow when it flows through a tube with convergent and divergent structures. Using this relationship, an American hydraulic engineer, Clemens Herschel, designed the first commercial Venturi meter in 1887. Due to its simple structure, high accuracy and low cost, the Venturi meter became one of the most commonly used flow meters in industries. Meanwhile, there is a long history for the research on Venturi meter for gas–liquid flow.[2,3] Owing to the complexity of two-phase flow, the research on the flow characteristics of gas–liquid flow going through Venturi meters still draws significant attentions today. At present, the common method for studying Venturi meter on wet gas flow in industry is to establish model based on the over reading theory. When the flow rate of the liquid phase is identified, the flow rate of the gas phase can be calculated using the over reading model and the differential pressure of the Venturi meter.

In 1962, Murdock[4] developed the classic over reading model for Orifice plate which was seem to be the foundation for the over reading models proposed subsequently. In 1967, Chisholm[5] acquired the form of wet gas over reading model for the orifice plate by assuming that the two phases of wet gas flow have the same contraction coefficient, but one of coefficients of the model was not been fixed. In 1977, by

Correspondence concerning this article should be addressed to Y. Xu at xuying@tju.edu.cn.

referring to the data of Thom's two-phase flow experiment at the pressure of 1.15 MPa, Chisholm[6] developed the influencing over reading model entirely. In 1997, de Leeuw[7] developed an over reading model for Venturi which reserves the main form of Chisholm's model but considering the influence of gas Froude number on the over reading of Venturi meter. In 2002, Steven[8] fit an over reading model with a new form using the wet gas data of National Engineering Laboratory. As all the mentioned above models were developed for the traditional one pair pressure tapings throttling device, the flow rate of gas phase can be calculated using these over reading models only under the circumstances where the flow rate of liquid phase is known. However, unfortunately, this information can virtually be acquired in industries easily. Consequently, researchers started to investigate a real two-phase flow meter that can be used in industries directly.

In recent years, researchers tend to use the multidifferential pressure signals to establish a model to solve the two flow rates of wet gas flow. In 2009, by employing the differential pressure and the total pressure loss of Venturi, Reader-Harris[9] proposed a method to calculate the flow rate of gas phase under the condition where none of the flow rate of wet gas flow is known. This work was adopted by International Organization for Standards (ISO) and released as an ISO technical report in 2012.[1] Most of the models are capable of generating acceptable results within the range of the data used to build them up, whereas due to the over reading theory that ignores the details of the wet gas flow, the extrapolation of these models are highly likely to produce significant biases.[10] Meanwhile, the theoretical researchers are exploring a model, which is derived from theories and can widely be applied to different scenarios. However, there is no such a method that can be used to identify two-phase flow rates reversed from a model based on two-phase hydrokinetics theories.

In this study, based on the hydrokinetics theory of the wet gas two-phase flow, the factors that affect the pressure loss of gas phase are discussed in the different sections of Venturi meters. Compared with the experimental results, the deviation of pressure loss predicted by the model for the standard Venturi meters with two diameter ratios was within an acceptable range. This study forms the foundation for establishing the measurement model of Venturi meter which can be further applied to wider conditions.

Wet Gas Pressure Drop Model for Venturi

Given the inherent complexity of the two-phase flow, it is necessary to propose an assumption for simplifying the research subject before the model was developed, namely there is only one static pressure value that exists in each individual cross section of the pipe. This study is limited to the analysis of the gas phase and it is assumed that the static pressure is the one of the cross section of the pipe. According to the assumption, it can be identified that this model belongs to the typical one-dimensional model.

As depicted in Figure 1, there are three major sections between the pair of pressure tapings of a standard Venturi meter: the straight tube in the front of the convergent section, the convergent section, and the throat. This model analyzes the pressure drop of gas phase in the three parts successfully.

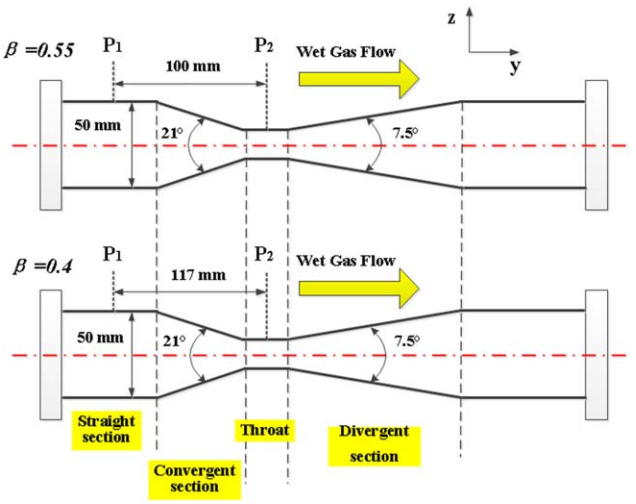

Figure 1. Two types of standard Venturi geometry.

[Color figure can be viewed in the online issue, which is available at wileyonlinelibrary.com.]

The flow patterns of the wet gas have been researched for decades.[11,12] By analyzing the velocity of the gas phase and the liquid flow rate, in ISO/TR11583, the flow patterns of wet gas were classified into four types including stratified flow, annular flow, mist flow, and slug flow.[1] In this technical report, the stratified flow was defined as the regime in which the free liquid runs along the bottom of the pipe with the gas flowing on the top of the pipe, and the definition of annular flow was the regime in which the liquid flows around the pipe wall with the gas flowing through the center of the pipe. However, in real flow regimes, in addition to the characteristics mentioned in the definitions above, the entrainment which will be defined in the section of "the model of entrainment" can be found in the pipes frequently. As a result, in this study, the uniform model for these two common types of flow regimes with the entrainment was developed.

For a stable horizontal two-phase flow, there are three factors affecting the change of static pressure of the gas phase:

1. The friction between the gas and the wall which depends on the roughness of the pipe and the Reynolds number for the gas phase.

2. The friction between the gas and the entrained droplet of liquid, which depends on the size of the droplet and the velocity discrepancies between them.

3. The friction between the liquid film and the gas core. For this factor, most researchers still describe it using the form of Darcy or Fanning equation both of which are for the single phase but they used their own ways to form the friction factor.[13]

As there is a convergent section within the Venturi tube, in addition to the factors mentioned above, the accelerate pressure drop resulting from the change of the circulation area should also be addressed. As a result, the differential form of the pressure drop of the wet gas flow through a horizontal Venturi tube can be expressed as

$$-dp=\frac{W_G}{A}dU_G+\frac{W_{LE}}{A}dU_D+\frac{\tau_{GW}S_{GW}}{A}dy+\frac{\tau_i S_i}{A}dy \qquad (1)$$

The left side of the equation depicts the change of the gas pressure drop within the dy distance of the axial wise of the tube. On the right side, the first term represents the

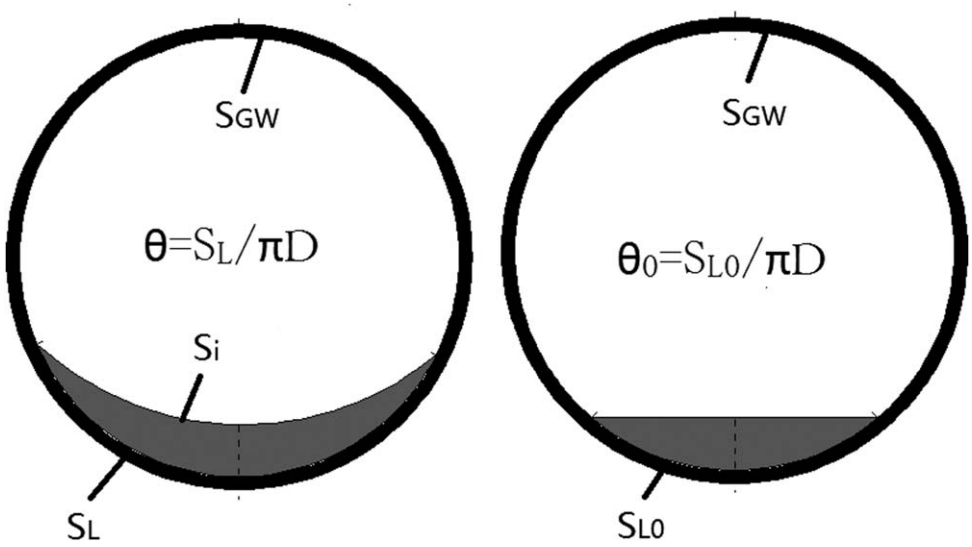

Figure 2. Schematic representation of wet gas in cross section of pipe.

(The left and right schematics represent the cross section with the actual wetted perimeter and the minimum attainable wetted perimeter, respectively.)

acceleration pressure drop of the gas, and the second one represents the entrainment pressure drop. The last two terms of the right side denote the frictional pressure drops of the gas which is caused by the wall of the tube and the liquid film, respectively. In this equation, W_G denotes the mass flow rate of gas phase and A is the actual circulation area of gas. U_G and U_D represent the local velocities of the gas and the entrained droplet, respectively. τ_{GW} and τ_i denote the shear stress between gas and wall and the one between gas and liquid film. S_{GW} represents the portion of the pipe perimeter in contact with the gas phase, and S_i is the contacted length between the two phases on the local cross section. The models for solving the four terms on the right side of the equation will be created in the proceeding sections.

The model of the wet perimeter

Before solving the two frictional pressure drops, there is a need to obtain the two perimeters (S_{GW} and S_i) and the two shear stresses (τ_{GW} and τ_i).

In 1989, taking the conversion between the potential and kinetic energies of the liquid phase into account, Hart et al.[14] modeled the wetted perimeter in the local cross section of horizontal pipes successfully. In 1997, Grolman and Fortuin[15] improved Hart's model and developed a set of methods for calculating the pressure drop of wet gas in the horizontal and inclined pipes which were entitled MARS model. The factors that affect the static pressure drop of the two phases in the straight pipes were considered in MARS model, and the predicted results were verified by the data collected from different experimental conditions satisfactorily. Given the above reasons, the approach for determining S_i in MARS model was adopted

$$S_i=\left[\frac{\theta-\theta_0}{1-\theta_0}\alpha^{0.5}+\frac{1-\theta}{1-\theta_0}\frac{\sin(\pi\theta_0)}{\pi}\right]\times\pi D \tag{2}$$

In Eq. 2, θ_0 and θ denote the minimum attainable wetted perimeter fraction and the actual one, respectively. α is the local void fraction and D is the diameter of the pipe. In MARS model, θ_0 can be approximated without generating significant accuracy loss using Eq. 3 and θ can be calculated using Eq. 4 after θ_0 is determined. The gas-phase Froude number Fr_G and the liquid-phase Weber number We_{LS} which correlates with θ are represented by Eqs. 5 and 6, respectively. Some of the parameters are described in Figure 2

$$\theta_0=0.624\times(1-\alpha)^{0.374} \tag{3}$$

$$\theta=\theta_0\left({}^{\sigma_{water}}/_{\sigma}\right)^{0.15}+\frac{We_{LS}{}^{0.25}Fr_G{}^{0.8}\rho_G}{(\rho_L-\rho_G)} \tag{4}$$

In Eq. 4, We_{LS} and Fr_G are liquid-phase Weber number and gas-phase Froude number, respectively, and their definitions are given in Eqs. 5 and 6

$$Fr_G=\frac{U_{GS}^2}{\alpha^2 gD} \tag{5}$$

$$We_{LS}=\frac{\rho_L U_{LS}^2 D}{\sigma} \tag{6}$$

Since the gas phase just contacts with the liquid film and the wall of tube in stratified flow and uncompleted annular flow conditions, S_{GW} can be expressed as

$$S_{GW}=\pi D-S_i \tag{7}$$

The model of shear stresses

In 2003, Van Werven et al.[16] constructed a type of model for measuring the static pressure of wet gas flow when it through the convergent and divergent structures of Venturi meter. The model was validated using the experimental data within the pressure range of 1.5–9 MPa and the estimated results were considered to be acceptable. In this model, the effect of liquid entrainment is considered when the correlation of shear stress between gas core and liquid film is developed

$$\tau_i=\frac{1}{2}f_i(\rho_G+C_h)\times U_{GC}^2 \tag{8}$$

In Eq. 8, f_i is the frictional factor between the two phases, C_h represents the extra quantity of density resulting from the liquid entrainment quantity W_{LE}

$$C_h = {W_{LE}}/{(AU_{GC})} \tag{9}$$

As the entrainment liquid would exist in the gas phase, in Ref. 16, the form of velocity of gas core U_{GC}, is expressed as

$$U_{GC} = \frac{W_G}{A\rho_G} + \frac{W_{LE}}{A\rho_L} \tag{10}$$

In this study, considering the difference between the velocities of gas core and liquid film, Eq. 8 has thus been modified. Replacing the velocity of gas core U_{GC} in Eq. 8 with the difference between the velocities of gas core and liquid film, the shear stress can be expressed by Eq. 11

$$\tau_i = \frac{1}{2} f_i (\rho_G + C_h) \times (U_{GC} - U_i)^2 \tag{11}$$

Following the method in Ref. 16, the stress between gas core and wall of the tube can be depicted by Eq. 12

$$\tau_{GW} = \frac{1}{2} f_{GW} (\rho_G + C_h) \times U_{GC}^2 \tag{12}$$

In Eq. 11, U_i is the mean velocity of the surface of liquid film and its form is followed by the model in Ref. 14

$$U_i = \begin{cases} 1.8 \times U_{LS}/(1-\alpha) & Re_L < 2100 \\ U_{LS}/(1-\alpha) & Re_L \geq 2100 \end{cases} \tag{13}$$

As depicted in Eq. 13, U_i relates to the liquid-phase superficial velocity and void fraction of the pipe. The form of liquid-phase Reynolds number is identified by Eq. 14

$$Re_L = \frac{\rho_L U_{LS} D}{\mu_L \theta} \tag{14}$$

The model of frictional coefficients

The material of the Venturi tubes used in these experiments is stainless steel, and the result of detection of it indicates that the absolute roughness is 5.98 μm. As a result, the semiempirical correlation developed by Nikuradse[17] was used in this study to calculate the frictional coefficient f_{GW}

$$\frac{1}{2\sqrt{f_{GW}}} = 2\log_{10}\ (Re_G \times 2\sqrt{f_{GW}}) - 0.8 \tag{15}$$

In the two-phase flow, the Reynolds number was replaced by gas-phase Reynolds number, of which the form will be discussed in Eq. 18.

Wallis[18] is one of the early researchers who determine the friction coefficient between liquid film and gas by referring to Nikuradse's research on single-phase flow.[17] This approach has been adopted and modified by other researchers in the following decades.[14,15,19]

Colebrook equation[20] is one of the most important equations for studying the friction factor in single-phase flow. It applies to all turbulent flow conditions. Values of friction factor that it predicts are generally accurate to within 10–15% of experimental data.[21] The modified Colebrook equation which depicted as Eq. 16 was used to describe the friction factor between the two phases

$$\frac{1}{2\sqrt{f_i}} = -2\log_{10}\ \left(\frac{k}{3.7D} + \frac{2.51}{2Re_G\sqrt{f_i}}\right) \tag{16}$$

In the two-phase flow, on the interface of the two phases, k represents the absolute roughness owing to the surface wave of liquid film. The empirical correlation suggested by Hamersma and Hart[22] was used to determine k

$$k \approx \frac{2.3(1-\alpha)D}{4\theta} \tag{17}$$

For the same reason, in two-phase flow, the Reynolds number in Eq. 16 should be replaced with the gas-phase Reynolds number Re_G which can be determined using the empirical conclusion identified by Eck[23]

$$Re_G = \frac{\rho_G U_{GS} D}{\mu_G (1 - \theta + \frac{S_i}{\pi D})} \tag{18}$$

Substituting Eqs. 17 and 18 into Eq. 16, f_i can be solved, and similarly, substituting Eq. 18 into Eq. 15, f_{GW} can be solved. The two shear stresses τ_i and τ_{GW} can be determined by substituting f_i and f_{GW} into Eqs. 11 and 12, respectively.

The model for the pressure drop of liquid entrainment

First, the momentum equation for entrained droplets should be obtained. Assume that the mean diameter of a single droplet is d_D, and the volume of the single droplet can be expressed by Eq. 19

$$V_D = \frac{4}{3}\pi\left(\frac{d_D}{2}\right)^3 \tag{19}$$

If the velocity of the entrained droplet is U_D and ψ is the volume fraction of the droplet to the entire gas core, the total volume of the droplet through the gas core section per unit time is $AU_D\psi$. In this study, using the resistance equation for flow around a sphere, the drag force on a single droplet can be depicted in Eq. 20, in which C_D is the drag coefficient of the sphere resistance

$$F_D = \frac{1}{8} C_D \rho_G (U_G - U_D)^2 \pi d_D^2 \tag{20}$$

Multiplying F_D by the total number of droplets in the control volume, that is, $AU_D\psi/V_D$, while taking into consideration of the relative velocities between the gas phase and droplet, the total force on the control volume can be presented by Eq. 21

$$F_{DC} = \psi A \frac{3\rho_G C_D}{4d_D} \times |U_G - U_D|(U_G - U_D)U_D \tag{21}$$

When the flow field is steady, the differential equation for the momentum of the total control volume can be expressed as

$${d(A\psi \times \rho_L U_D^2)}\Big/{dt} = A\psi \times \rho_L U_D^2 \frac{dU_D}{dy} \tag{22}$$

According to the momentum theorem, Eq. 21 should be equal to Eq. 22. Thus, the momentum equation for the entrained droplet is

$$U_D \frac{dU_D}{dy} = \frac{3}{4} C_D \left(\frac{\rho_G}{\rho_L}\right) \frac{|U_G - U_D|(U_G - U_D)}{d_D} \tag{23}$$

The mean diameter of a single droplet d_D, in the equation above, can be estimated using the correlation as recommended by Azzopardi and Govan[24]

$$d_D = \lambda_T \left(\frac{15.4}{We'^{0.58}} + \frac{3.5\rho_G W_{LE}}{\rho_L W_G}\right) \tag{24}$$

Where, the Rayleigh–Taylor instability wavelength and other correlated parameters are presented in the following four equations (Eqs. 25–28)

$$\lambda_T = \sqrt{\frac{\sigma}{\rho_L g}} \tag{25}$$

$$We' = (\rho_L U_G^2 \lambda_T)/\sigma \tag{26}$$

$$C_D = \begin{cases} \dfrac{24}{Re_D}(1+0.15Re_D)^{0.687} & Re_D < 1000 \\ 0.44 & Re_D \geq 1000 \end{cases} \tag{27}$$

$$Re_D = \frac{\rho_G |U_G - U_D| d_D}{\mu_G} \tag{28}$$

Based on the above analysis, if W_{LE} and W_G are identified, the local value of dU_D/dy can be calculated using Eq. 23.

The model of accelerate pressure drop

For determining the term of accelerate pressure drop on the right side of Eq. 1, the actual velocity of gas phase should be calculated using the following continuity equation

$$\frac{dW_G}{dy} = 0 \tag{29}$$

In Eq. 29, with an independent void fraction model, U_G can be solved by a determined area of the local cross section for gas A.

In 2006, Woldesemayat et al. analyzed the 68 existing representative void fraction models in the research area of two-phase flow history.[25] These models were classified and verified by different sets of experimental data. The conclusions indicated that, for annular/mist flow in horizontal straight pipes, the model developed by Lockhart and Martinelli[26] was more suitable than others. However, it should be noted that, all models in Ref. 25 are the research for fully developed two-phase flow in straight pipes rather than for the flow in throttle devices. As a result, Eq. 30 should be modified

$$\alpha = \left[1+0.28\left(\frac{1-x}{x}\right)^{0.64}\left(\frac{\rho_G}{\rho_L}\right)^{0.36}\left(\frac{\mu_L}{\mu_G}\right)^{0.07}\right]^{-1} \tag{30}$$

To the best of our knowledge, unfortunately, there is no available void fraction model that is able to predict the two-phase information on the local cross section of convergent structure tubes. Therefore, the void fraction model was modified to fit the form of the following equation

$$\alpha = \gamma\left[1+0.28\left(\frac{1-x}{x}\right)^{0.64}\left(\frac{\rho_G}{\rho_L}\right)^{0.36}\left(\frac{\mu_L}{\mu_G}\right)^{0.07}\right]^{-1} \tag{31}$$

In Eq. 31, x is the quality and γ represents the corrected coefficient which is defined as the linear equation of Lockhart–Martinelli parameter X which was defined by Eq. 33

$$\gamma = \kappa X + 1 \tag{32}$$

$$X = \frac{W_L}{W_G}\sqrt{\frac{\rho_G}{\rho_L}} \tag{33}$$

In addition, due to the convergent structure in a Venturi tube, there will be a blocking effect for the liquid phase and then, the proportions of liquid distribution will be much more than what was in straight pipes. By contrast, when there is no liquid in pipe, the void fraction model should regress to the situation of $\alpha = 1$. Given the above two factors, the form of Eq. 32 is determined.

In comparison to the two types of Venturi with different diameter ratios, the multiplier of Lockhart–Martinelli parameter, κ, is fit respectively with the form of the following equation in which the effects of pressure and gas flow rate were taken into account. Owing to κ being a dimensionless coefficient, the forms of the factors mentioned previously are proposed by $\rho_G \rho_L^{-1}$ and $U_{SG}(gD)^{-1/2}$ groups, respectively

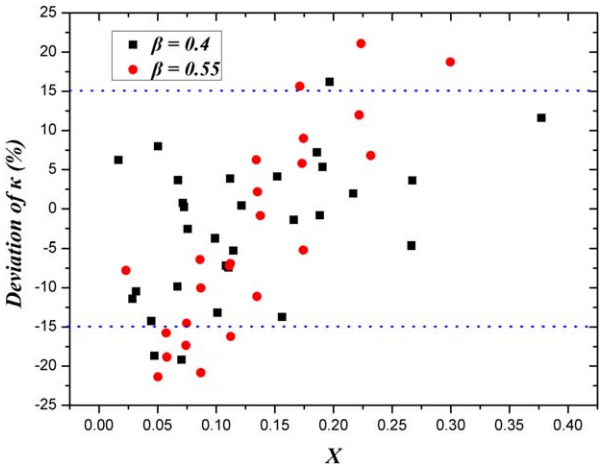

Figure 3. Deviation of κ for different diameter ratios.

[Color figure can be viewed in the online issue, which is available at wileyonlinelibrary.com.]

$$\kappa = \begin{cases} -0.0138\left(\frac{\rho_G}{\rho_L}\right)^{0.4413}\left(\frac{U_{SG}}{\sqrt{gD}}\right)^{2.5056} - 0.7949 & \beta = 0.4 \\ -0.1259\left(\frac{\rho_G}{\rho_L}\right)^{-0.0234}\left(\frac{U_{SG}}{\sqrt{gD}}\right)^{0.8743} - 0.1439 & \beta = 0.55 \end{cases} \tag{34}$$

The relative deviations of the fit coefficient κ, for different diameter ratio, are plotted in Figure 3. For the diameter ratio of 0.4 and 0.55, 90% and 78% of the test points are within the error band of $\pm 15\%$, respectively. The deviations indicate that the accuracy of the fitting work is far from excellent. However, in this model, these deviations will not induce an unacceptable result in static pressure calculation which can be proved in the proceeding sections.

As discussed previously, the motion of droplet was addressed using its momentum equation. However, as the momentum equation of the gas phase contains the information of static pressure, this approach is not applicable to discuss the gas-phase velocity. In fact, Eq. 1 is the momentum equation for the gas phase. As a result, using Eq. 1, the pressure of gas phase can be calculated after determining the gas velocity and other terms on the right side of Eq. 1. Given this, an independent correlation for void fraction should be used in this model.

The model of entrainment

As the quantity of entrained droplet, W_{LE} was used in the above models, there is a need to develop a model to determine it. As depicted in Eq. 34, the definition of entrainment is dividing W_{LE} by the total liquid flow rate W_L

$$E = {}^{W_{LE}}\!/_{W_L} \tag{35}$$

In 2001, Pan and Hanratty[27] indicated that entrainment is resulted from a balance between the rate of atomization of the liquid layer flowing along the pipe wall and the rate of drop deposition. In their study, two approaches that were summarized based on both experimental and theoretical analyses for predicting the quantity of entrained liquid in annular

flow were developed. Due to its accuracy and convenience, the semiempirical approach was cited in this study. Equation 36 depicts the main empirical correlation for entrainment E in which a and n are both constant. d_{32} is the Sauter mean diameter of the droplet which can be presented using Eq. 37

$$\frac{E/E_m}{1-(E/E_m)} = a\left(\frac{DU_G^3\rho_G^{0.5}\rho_L^{0.5}}{\sigma}\right)\left(\frac{\rho_G^{1-n}\mu_G^n}{d_{32}^{1+n}g\rho_L}\right)^{1/2-n} \tag{36}$$

$$\left(\frac{\rho_G U_G^2 d_{32}}{\sigma}\right)\times\left(\frac{d_{32}}{D}\right) = 0.0091 \tag{37}$$

Equation 38 defines the maximum entrainment E_m and W_{LFC} is the critical film flow below which atomization does not occur

$$E_m = 1 - \frac{W_{LFC}}{W_L} \tag{38}$$

Equation 39 is the fit correlation of the critical Reynolds number for liquid film Re_{LFC}, in which ω represents a parameter determined by Eq. 40

$$Re_{LFC} = \frac{4W_{LFC}}{\mu_L \pi D} = 7.3(\log_{10}\varpi)^3 + 44.2(\log_{10}\varpi)^2 - 263(\log_{10}\varpi) + 439 \tag{39}$$

$$\varpi = \frac{\mu_L}{\mu_G}\sqrt{\frac{\rho_G}{\rho_L}} \tag{40}$$

Substituting Eq. 40 into Eq. 39, W_{LFC} is obtained and the entrainment E can be determined by substituting Eqs. 37 and 38 into Eq. 36.

In addition, when the wet gas flow enters the throat section of a Venturi, there will be some extra liquid film that is entrained into the gas core.[24,28] To determine the extra entrainment ΔE_f, the following correlations developed in Ref. 16 were used

$$\Delta E_f = 1 - 1.063\left(\frac{We_c}{We}\right)^{0.34} \tag{41}$$

$$We_c = 0.1857\times(90 - \theta/2) - 5.17 \tag{42}$$

$$We = \frac{\rho_G U_{SG}^2 m}{\sigma} \tag{43}$$

As depicted in Eq. 41, ΔE_f is correlated with the structure of the Venturi tubes and several flow parameters. σ is the surface tension and m is the mean thickness of liquid film which can be obtained by using Eq. 44

$$m = (1-\alpha)\frac{D}{4\theta} \tag{44}$$

Equations 41–44 can be used to develop the model for solving the extra entrainment ΔE_f.

In addition to the factors mentioned above, there are a few processes that may influence the variation of static pressure of the gas. In 1997, Azzopardi[29] summarized the researches on the behavior of droplets and liquid film in annular two-phase flow over the past decades and reviewed these researches. The two mechanisms of atomization, namely, bag break up and ligament break up were defined in his research.

The process of atomization coursing the break up of the entrained liquid will induce an extra pressure loss due to the acceleration procedure of the smaller drops. It is worth

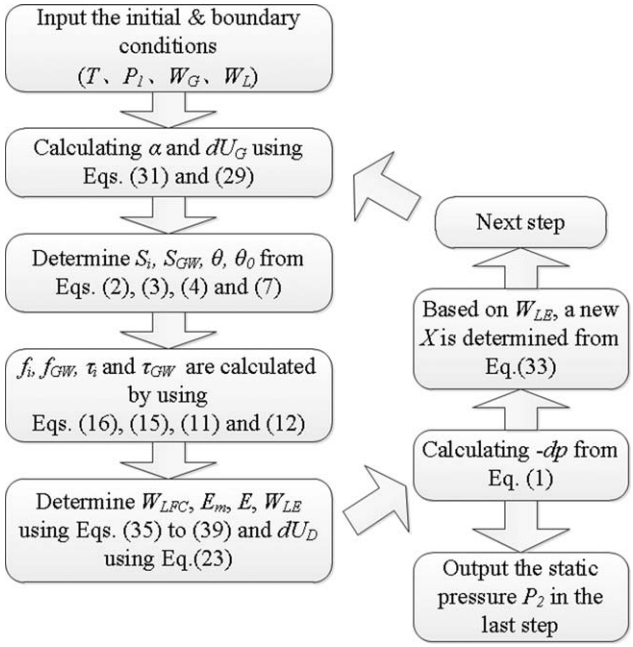

Figure 4. Flow chart of the model for static pressure distribution calculation of wet gas.

studying droplet behavior and evolutionary process as the trends of two-phase flow research heavily rely on the development of the real flow field movement focusing on fine details. However, most of the models and equations merely described the specific database qualitatively and none of them can be used to calculate the pressure drop by only using the macroscopic parameters such as temperature, line pressure, and so forth. Consequently, further researches on this subject are required and the effect of atomization cannot be directly expressed in this model for the present.

Summary of the models

Integrating the models presented above, a set of models for calculating the axial static pressure of wet gas in Venturi was developed. When the two phases flow rates and the inlet pressure are known, considering the factors related, the static pressure in local cross sections can be obtained by solving the momentum equation for the gas phase. The interfacial perimeter is determined by Eq. 2 and the shear stresses are calculated from Eqs. 11 to 16. The pressure drop term of friction can be determined using these two parameters. The pressure loss of acceleration is obtained by determining the void fraction which can be calculated from Eq. 31. For the pressure drop of entrainment, the related parameters including the local entrainment and the velocity of the droplets are calculated using Eqs. 35 and 36 and 23, respectively. On obtaining the above three major pressure loss factors, the static pressure of gas phase in the local step can be calculated from Eq. 1 accordingly. The procedures were implemented iteratively by taking the results of the previous step to be the initial conditions of the next one. The detail of the calculation procedure is plotted in Figure 4 and this model was compiled into a MATLAB computer program. As the model is less dependent on the specific empirical apparatus and data, it provides the basis for further establishing a flow measurement model of wet gas which will produce fewer biases when it is extrapolated. Figure 4 is the flow chart for the calculation of gas-phase static pressure.

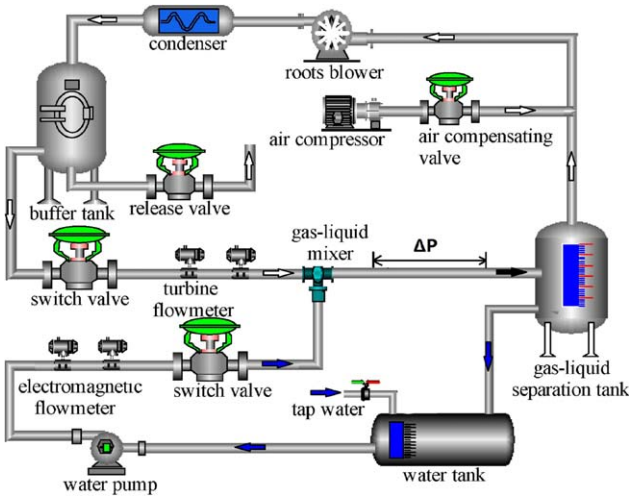

Figure 5. Schematic diagram of the experimental setup.

[Color figure can be viewed in the online issue, which is available at wileyonlinelibrary.com.]

The Experiment Setup

The experiments were conducted on the dual-closed recirculating loop wet gas test facility at Tianjin University, China. The test mediums of fluids were air and water. The gas flow is produced by a Roots blower, and is capable of delivering volumetric flow rates of 1–1000 m^3/h at the line pressures ranging from 0.1 to 1.6 MPa gauge. With the uncertainty of 1%, a 100 mm turbine meter was used to measure the reference dry gas flow rate. The liquid (water) was injected into the stream via an injector nozzle placed on the axis of the pipe, facing downstream. A water pump was used to deliver liquid to the nozzle at the flow rate up to 8 m^3/h. The liquid flow rate through the nozzle was controlled via a 25-mm ball valve, which was located on the liquid recirculating loop. The reference liquid flow rate is measured by an electromagnetic meter, for which the uncertainty was 0.5%. The horizontal mixture test section was located on the downstream of the injector nozzle, the inner diameter of which is 50 mm. Using the gas–liquid separation tank, the two-phase fluids were circulated back to their own loop (Figure 5).

Two 50 mm standard Venturi meters with the diameter ratios of 0.55 and 0.4, respectively, were chosen to be in the experiments. The experiments were implemented at five different line pressures, which were 0.1, 0.21, 0.3, 0.39, and 0.6 MPa. The gas flow rates, expressed by the superficial velocity (U_{GS}), were selected in the range between 3 and 12 m/s. In Lockhart–Martinelli terms, the liquid flow rates correspond to 0–0.2 for all conditions. The range of the liquid volume fraction (LVF) of the two-phase flow is 0–1.96%.

Table 1. Scope of the Experiments

β	Line Pressure (MPa)	U_{GS} (m/s)	X	U_{LS} (m/s)	T (°C)	LVF (%)
0.55	0.21	6–12	0–0.2	0–0.17	12.9–16.9	0–1.39
	0.39	6–12	0–0.2	0–0.21	13.5–17.7	0–1.72
	0.6	3–10	0–0.2	0–0.18	18.6–21.1	0–1.79
0.4	0.1	6–12	0–0.2	0–0.16	14.5–17.9	0–1.31
	0.3	6–12	0–0.2	0–0.18	13.1–17.9	0–1.96

The flow conditions of the experiments are summarized in Table 1.

Results and Discussion

The horizontal distances between the pressure taps of the two types of Venturi meters are 99 mm (for $\beta = 0.55$) and 116 mm (for $\beta = 0.4$), respectively. As the step length was set to be 1 mm in stream-wise, the total numbers of steps for the two types of prototypes are 100 and 117. Assuming that the pipe diameter is constant within a step length, the boundary condition of the model can be determined. Using the calculation procedures discussed previously, the flow parameters can be obtained in the first step. By setting the results of the previous step to be the initial conditions of the next one, the calculation procedures was continued until the static pressure of the throat tap was obtained.

Figure 6 depicts the pressure drop distribution in stream-wise calculated by the model for the Venturi with the diameter ratio of 0.55 at certain experimental condition. As shown on the right side of Eq. 1, the three terms which consist of the total pressure drop are also presented in Figure 6. The abscissa is the axial distance between the upstream and throat taps of the Venturi meter, and the ordinate denotes the pressure drop from the upstream tap. The modeling result indicated that, in wet gas flow, the major factor that affects the total pressure drop is the accelerate pressure drop due to the variation of the gas flow area. This situation was consistent with the throttling design in the convergent section of the Venturi meter. Although the real flow area of the gas phase in the cross section was affected by the thickness of the local liquid film, the main trend of throttling in the convergent section is unchangeable. However, in the straight section and throat, there is virtually no change in the pressure drop of acceleration as the cross section of pipe is constant in these sections. The frictional pressure drop is the second major influential factor for the total pressure drop, even though the quantity of which is much more less than the one of accelerate pressure drop. There is little variation of the frictional pressure drop in the zone of y less than 0.05 m, however, its quantity increases dramatically when y is more than 0.8 m. Its profile indicated that, in the straight

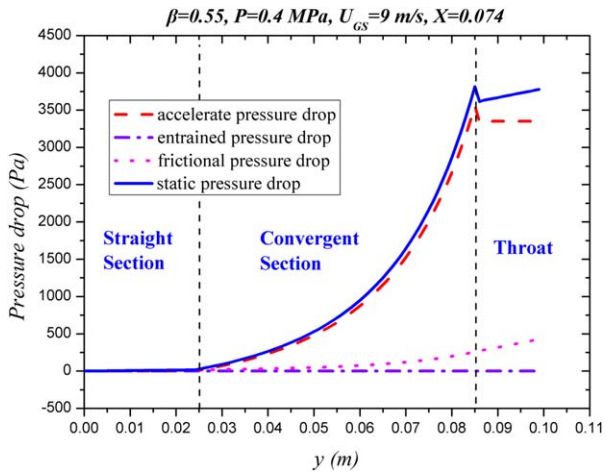

Figure 6. Axial distribution of the pressure drop terms in the Venturi ($\beta = 0.55$).

[Color figure can be viewed in the online issue, which is available at wileyonlinelibrary.com.]

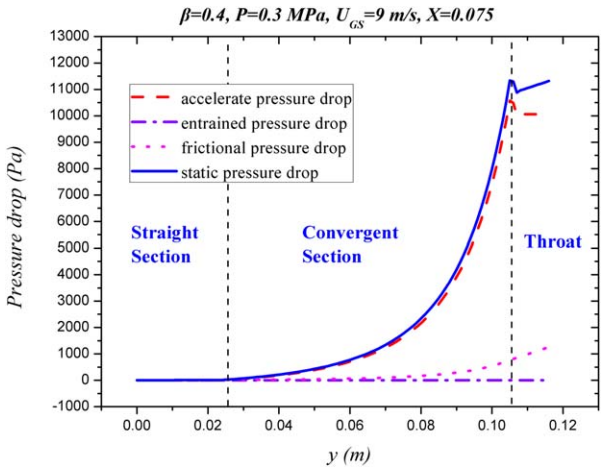

Figure 7. Axial distribution of the pressure drop terms in the Venturi ($\beta = 0.4$).

[Color figure can be viewed in the online issue, which is available at wileyonlinelibrary.com.]

section, the velocities of gas core and liquid film were both stable and the surface fluctuation of the film was in a relatively low level. Due to the variation of the pipe diameter and the acceleration of gas phase, the intensity of the surface fluctuation of the film increased, leading to the stronger induced friction effect between the two phases in the convergent section. In the throat, the total pressure drop was largely contributed by the frictional term. In addition, the pressure drop coursed by entrainment has little influence on the total one in the three sections. Despite the fact that the quantity of the entrained term increases by several dozens of Pascal in the convergent section and throat, the effect of which seems insignificant when comparing with the other two factors. This phenomenon can be explained as, even though the entrainment widely exists in most parts of the Venturi meter, there is little friction between the entrained droplets and the gas phase, that is, the droplets will be accelerated to the velocity nearly equal to the gas velocity in a short time.

Figure 7 shows the distribution of the total pressure drop and its three components in the Venturi with the diameter ratio of 0.4. To compare the calculated data with that shown in Figure 6, the data in similar experimental conditions along with the line pressure is plotted in Figure 7. The remarkable difference between the pressure drop distribution of the two types of Venturi is that, for the 0.4 prototype, the static pressure loss (about more than 11,000 Pa) is much greater than that reflected in the 0.55 one (about less than 4000 Pa), even though the line pressure in Figure 7 is merely 0.3 MPa. This phenomenon indicates that the decisive factor affecting the total pressure drop of wet gas in Venturi, in the same pipe diameter, is the diameter ratio. It is totally consistent with Bernoulli's theorem for the gas phase. The quantity of all three pressure drop terms in Figure 7 increases, however, the proportion of their contribution to the total pressure loss in every section of Venturi is similar to the result indicated in Figure 6. It confirms that the distribution trend of the pressure drop factors for different types of Venturi meters can be considered to be identical.

A more detailed experiment for measuring the pressure change along the Venturies in different orientations was carried out by Azzopardi et al.[30] in 1989. In that work, the pressure tapings were provided along each Venturi spaced at 0.01-m intervals. As the geometry of the Venturi meters used in that work differs from the ones used in this study, the predicted results in this study cannot be compared with the experimental data in that work directly. Whereas the trend of the pressure difference in the convergent section of the both works are similar. Owing to the much greater constriction of the Venturi meters used in Azzopardi's work, the peak pressure drops represented in that experiment become greater than that in this study for a given superficial gas velocity. Special attention should be paid to the less pressure loss in the throat indicated in Azzopardi's work. The reason for this phenomenon could probably lie in the less entrainment in this section due to the smaller throat diameter. In general, more experiments are needed to test the validity of this model in the section between the two present pressure tapings.

Using the Venturi meter with the diameter ratio of 0.4, Figure 8 plots the predicted static pressure profiles and the experimental data under the conditions of 0.1 MPa and different liquid fractions. With the increase of the liquid fraction in wet gas, there was a significant increase in the pressure drop. It is also noted that the performance of the static pressure was distinct from different sections of the Venturi. As discussed previously, the pressure drop generated primarily in the convergent section for all conditions, whereas, the variation of it was relatively fewer in the other sections. In the throat of the Venturi, the static pressure was highly sensitive to the variation of the liquid fraction, that is, the more the liquid present in wet gas, the larger will be the value of the pressure drop. At the meantime, as the presence of the liquid phase, the loss of head of gas at the entrance of the throat was greater than the entrance loss with total gas flow. The similar trend showing the more liquid holdup will produce more entrance loss can be found in Figure 8. However, in the straight section, the performance of pressure profile seems to be irrelevant to the liquids. The distributions of the pressure loss factors in Figures 8 and 9 indicate that, when wet gas through Venturi, the total pressure drop is largely caused by the squeeze effect on the gas phase in the convergent section due to the presence of liquid. In Figure 9, the pressure profiles of the wet gas through the 0.55 Venturi under different liquid fractions are plotted. As the trend of these profiles is similar to that of the profiles shown in Figure 8, the mechanism of pressure drop

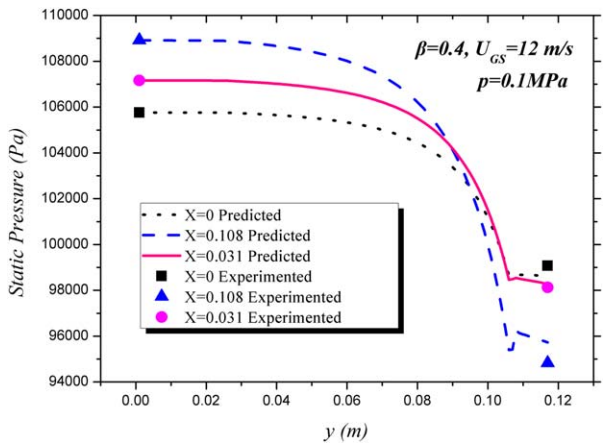

Figure 8. Predicted pressure drop and tested data in Venturi ($\beta = 0.4$) with different liquid fraction.

[Color figure can be viewed in the online issue, which is available at wileyonlinelibrary.com.]

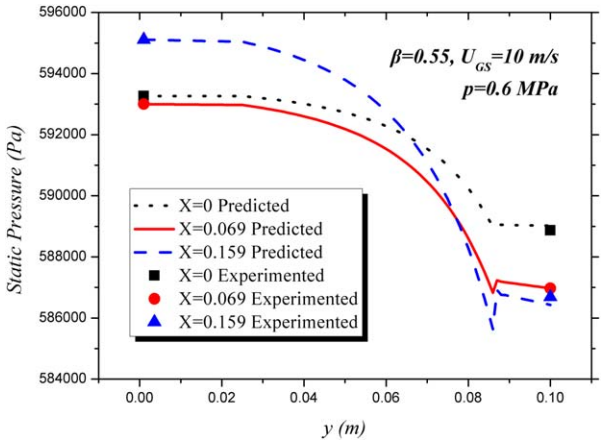

Figure 9. Predicted pressure drop and tested data in Venturi ($\beta = 0.55$) with different liquid fraction.

[Color figure can be viewed in the online issue, which is available at wileyonlinelibrary.com.]

generation in different types of Venturi meters can be considered to be the same.

Figures 10 and 11 illustrate the relative deviation of the pressure drops predicted by the models against to the Venturi meters with the diameter ratio of 0.4 and 0.55, respectively, in different line pressures. Both of the two plots are demonstrated as the relative deviation of the pressure drops against the liquid loading which is expressed as the Lockhart–Martinelli parameter. All the relative deviations of the test points are within ±15%. For the $\beta = 0.4$ Venturi, in Figure 10, the error of 88% predicted points were within ±10%. For $\beta = 0.55$ Venturi, the percentage of the estimated points within the same error band is 94.3%. The standard deviation of the pressure drop for the 0.4 and 0.55 Venturi meters are 7.577 and 2.486, respectively. The applicability of the model for these two Venturi meters within the line pressure rang of 0.1–0.6 MPa can thus be confirmed. The error can be attributed to the capability of the model in analyzing detailed mechanisms of the complicated two-phase flow in Venturi meters being limited. As the factors that influence the static pressure of wet gas are not taken into consideration, therefore,

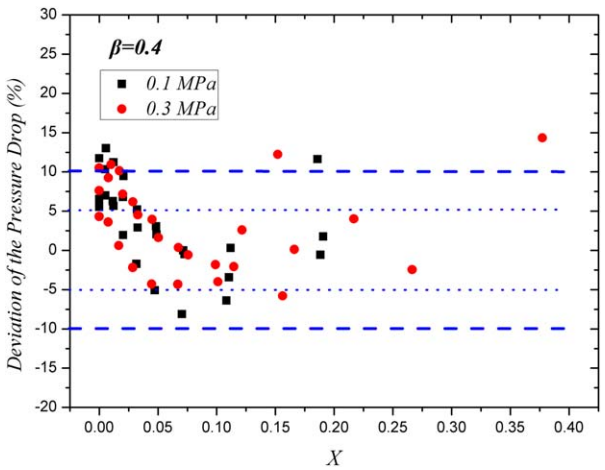

Figure 10. Deviation of the predicted pressure drop in Venturi ($\beta = 0.4$) with different line pressures.

[Color figure can be viewed in the online issue, which is available at wileyonlinelibrary.com.]

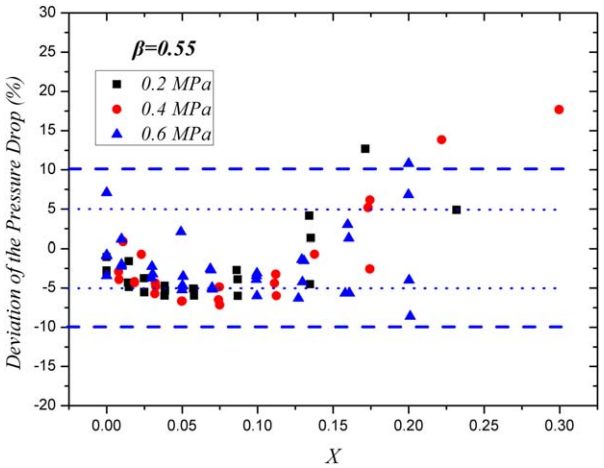

Figure 11. Deviation of the predicted pressure drop in Venturi ($\beta = 0.55$) with different line pressures.

[Color figure can be viewed in the online issue, which is available at wileyonlinelibrary.com.]

further efforts should be made on understanding the wet gas flow in the pipe with convergent and divergent structure.

Conclusion

Using the theory of hydrodynamics, the wet gas flow in two horizontal Venturi meters was analyzed. The model for calculating the axial distribution of the wet gas static pressure in the Venturi meters has been developed, which takes into consideration the factors including the void fraction, the friction between the two phases and the entrainment. For validating the developed model, the wet gas experiments were carried out under the pressure range of 0.1–0.6 MPa using the two types of Venturi meters. The predicted results, in comparison to the corresponding experimental data, fall into a reasonable range. As the mechanism of the wet gas flow in Venturi meter was discussed, this study provides the basis for further establishing a flow measurement model of wet gas which will produce fewer biases when it is extrapolated.

Acknowledgments

The authors acknowledge the financial support of the National Nature Science Foundation of China (No. 60974118) and National Hi-Tech Research and Development Program (863 Program) (No. 2007AA04Z180).

Literature Cited

1. ISO. ISO/TR 11583 Measurement of Wet Gas Flow by Means of Pressure Differential Devices Inserted in Circular Cross-Section Conduits, 1st ed. Switzerland: ISO, 2012.
2. Spialter M. *Characteristics of Two Phase Flow through a Vertical Venturi*. New York, America: D. Eng. Sc. thesis in Mechanical Engineering, New York University; 1952.
3. Bizon E. *Two-Phase Flow Measurement with Sharp-Edged Orifices and Venturis*. Chalk River, ON: Atomic Energy of Canada Ltd., 1965.
4. Murdock J. Two-phase flow measurement with orifices. *J Fluids Eng*. 1962;84(4):419–432.
5. Chisholm D. Flow of incompressible two-phase mixtures through sharp-edged orifices. *J Mech Eng Sci*. 1967;9(1):72–78.
6. Chisholm D. Research note: two-phase flow through sharp-edged orifices. *J Mech Eng Sci*. 1977;19(3):128–130.

7. De Leeuw R. Liquid correction of Venturi meter readings in wet gas flow. Paper presented at: North Sea Flow Measurement Workshop 1997; Kristiansand, Norway.
8. Steven R. Wet gas metering with a horizontally mounted Venturi meter. *Flow Meas Instrum.* 2002;12(5):361–372.
9. Reader-Harris M, NEL T, Graham E. An improved model for venturi-tube over-reading in wet gas. Paper presented at: 27th International North Sea Flow Measurement Workshop; 20–23 October, 2009; Tønsberg, Norway.
10. De Leeuw R, Steven R, Van Maanen H. Venturi Meters and Wet Gas Flow. Paper presented at: North Sea Flow Measurement Workshop; 25–28 October, 2011; Tønsberg, Norway.
11. Baker O. Simultaneous flow of oil and gas. *Oil Gas J*. 1954;53(3): 185–190.
12. Mandhane J, Gregory G, Aziz K. A flow pattern map for gas—liquid flow in horizontal pipes. *Int J Multiphase Flow*. 1974;1(4):537–553.
13. Lide F, Tao Z, Ying X. Venturi wet gas flow modeling based on homogeneous and separated flow theory. *Math Probl Eng*. 2008; 2008.
14. Hart J, Hamersma P, Fortuin J. Correlations predicting frictional pressure drop and liquid holdup during horizontal gas-liquid pipe flow with a small liquid holdup. *Int J Multiphase Flow*. 1989;15(6): 947–964.
15. Grolman E, Fortuin JM. Gas-liquid flow in slightly inclined pipes. *Chem Eng Sci*. 1997;52(24):4461–4471.
16. Van Werven M, Van Maanen H, Ooms G, Azzopardi B. Modeling wet-gas annular/dispersed flow through a Venturi. *AIChE J*. 2003; 49(6):1383–1391.
17. Nikuradse J. *Laws of Flow in Rough Pipes*. Washington: National Advisory Committee for Aeronautics, 1950.
18. Wallis GB. *One-dimensional two-phase flow*. McGraw-Hill; 1969.
19. Schubring D, Shedd T. A model for pressure loss, film thickness, and entrained fraction for gas–liquid annular flow. *Int J Heat Fluid Flow*. 2011;32(3):730–739.
20. Colebrook CF. Turbulent flow in pipes, with particular reference to the transition region between the smooth and rough pipe laws. *J ICE*. 1939;11(4):133–156.
21. Daugherty RL, Franzini JB. *Fluid Mechanics, with Engineering Applications*. New York: McGraw-Hill, 1977.
22. Hamersma P, Hart J. A pressure drop correlation for gas/liquid pipe flow with a small liquid holdup. *Chem Eng Sci*. 1987;42(5):1187–1196.
23. Eck B. *Einführung in die technische Strömungslehre*. Berlin, Germany: Springer; 1936.
24. Azzopardi B, Govan A. The modelling of Venturi scrubbers. *Filtr Separat*. 1984;21:196–200.
25. Woldesemayat MA, Ghajar AJ. Comparison of void fraction correlations for different flow patterns in horizontal and upward inclined pipes. *Int J Multiphase Flow*. 2007;33(4):347–370.
26. Lockhart R, Martinelli R. Proposed correlation of data for isothermal two-phase, two-component flow in pipes. *Chem Eng Prog*. 1949; 45(1):39–48.
27. Pan L, Hanratty TJ. Correlation of entrainment for annular flow in horizontal pipes. *Int J Multiphase flow*. 2002;28(3):385–408.
28. Fernandez Alonso D, Azzopardi B, Hills J. Gas/liquid flow in laboratory-scale Venturis. *Process Saf Environ Prot*. 1999;77(4):205–211.
29. Azzopardi B. Drops in annular two-phase flow. *Int J Multiphase Flow*. 1997;23(7):1–53.
30. Azzopardi B, Memory S, Smith P. Experimental study of annular flow in a Venturi. *Proceedings of the 4th International Conference on Multiphase Flow*. Nice, 1989.

Manuscript received May 5, 2014, and revision received July 1, 2014.